

Original Article: Synthetic Impatienol analogues as Potential Cyclooxygenase-2 Inhibitors: A preliminary study



Garima Sharma | S. B. Sharma*

Department of Chemistry, Faculty of Science, Motherhood University, Roorkee, Uttarakhand, India



Citation G. Sharma, S. B. Sharma*, **Synthetic Impatienol analogues as Potential Cyclooxygenase-2 Inhibitors: A preliminary study.** *J. Appl. Organomet. Chem.*, 2021, 1(2), 66-75.

<https://doi.org/10.22034/jaoc.2021.276815.1006>



Article info:

Received: March 8, 2021

Accepted: April 9, 2021

Available Online: April 19, 2021

ID: JAOC-2103-1006

Checked for Plagiarism: Yes

Peer Reviewers Approved by:

Dr. SUNIL V. GAIKWAD

Editor who Approved Publication:

Professor Dr. Abdelkader Zarrouk

Keywords:

Cyclooxygenase-2, Impatienol, Naphthoquinone, Molecular docking, Multiple receptor conformations.

ABSTRACT

Cyclooxygenase (COX) is a key enzyme in the biosynthetic pathway leading to the formation of prostanoids, including prostaglandins, prostacyclin and thromboxane, which are mediators of inflammation. COX-2, as undetectable normal tissues, and induced during inflammation, hypoxia and Wnt-signalling, is present in many cancers. A series of dimeric 2-hydroxy-1, 4-naphthoquinone analogs was designed and subsequently synthesized via single-step conversion of readily available aromatic aldehydes. All compounds were evaluated by cyclooxygenase-2 (COX-2) assays in vitro by surface plasmon resonance (SPR) to determine inhibitory potency. Compounds 1-10 showed moderate to good inhibition with K_d values ranging from $1.25 \times 10^{-6} \text{M}$ to $1.97 \times 10^{-10} \text{M}$ for COX-2. Diclofenac and nimesulide were taken as standard drugs to compare the results of the SPR assay. Mode of binding of most potent compound 10 ($K_d = 1.97 \times 10^{-10} \text{M}$) was further investigated by molecular docking studies. Multiple receptor conformations (MRC) of the binding site were generated to simulate the probable protein movement. The ensemble docking studies were carried out to analyze various interactions that lead to the binding.

Introduction

Cyclooxygenase-2 (COX-2) is one of the key enzymes in the modulation of inflammation and acts by catalyzing the rate-limiting step that leads to the formation of prostaglandins (PGs) from arachidonic acid. The inflammatory paradigm of COX-2 expression is defined aphysiological since it is part of a complex physiological self-regulating response to

pathological conditions, carried out by specific cell and tissue types. However, COX-2 expression may surpass normal physiological control, resulting in fatally pathological states, namely, autoimmune diseases and cancer [1]. In different examples of autoimmune diseases, such as rheumatoid arthritis [2], systemic lupus erythematosus [3] or some forms of diabetes [4], the hyperactivation of such subpopulations of immune cells is directly dependent on the over-expression of COX-2. The hyperexpression

*Corresponding Author: S.B.Sharma(deanscience18@gmail.com)

of COX-2 is the result of cross-talk between several mediators of inflammation, including interleukins and cytokines (i.e., IL-1, IL-6 and TNF α), and it occurs via transcriptional activation [5]. Moreover, COX-2 is constitutively expressed in several cancers [6].

Cox-2 is a homodimeric heme-containing protein with a molecular weight of 71 kDa. The COX molecule consists of three independent folding units: An EGF-like domain and the two functional domains. Within the enzymatic domain, the two functionalities, i.e. cyclooxygenase and peroxidase, are adjacent but spatially distinct. The COX active site in the protein interior is connected to the membrane

by a long non-polar channel through which the substrate/inhibitor gains access. The active site of cyclooxygenases (Figure 1) contains mainly hydrophobic residues [7].

The binding site of COX-2 (PDB-ID: 3ln1) [8] is about 23 Å (between Ser516:O γ and Asp501:O); with the deep cylindrical-shaped pocket being more expanded at the bottom. The affinity of selective COX-2 ligands is mainly governed by the hydrophobic interactions within the very confined COX-2 binding pocket as reported by Kurumbail *et al.*, studying the crystal structure of COX-2 bound with the selective COX-2 inhibitor SC-558 [9].

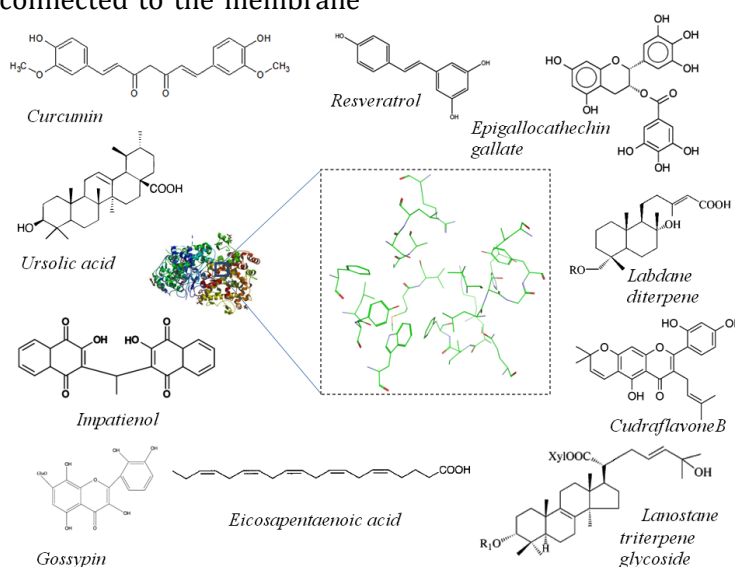


Figure 1. Structure of some known COX-2 inhibitors

Recently, Marc Diederich *et al.*, reviewed natural compounds affecting the expression of COX-2 [1] namely curcumin, resveratrol, epigallocatechin gallate, apigenin, genistein, kaempferol, chrysin, fisetin, sulforaphane, diallyl trisulfide, bromelain, schisandrin, mangiferin, and glucosamine. There are a plethora of natural compounds reported in the literature which inhibit COX-2 (Figure 1) like Curcumin [10], epigallocatechin gallate [11], resveratrol [12], fatty acid [13], ursolic acid [14], gossypin [15], Lanostane [16], labdane diterpenes [17], Cudraflavone B [18], piperidine alkaloid and Impatienol [19].

Kyoko Ishiguro *et al.*, observed significant selective cyclooxygenase-2 (COX-2) inhibitory activity with Na salt of impatiencia which was

isolated from the corolla of *Impatiens balsamina* L. (Balsaminaceae) [19]. Molecular docking studies conducted for a deeper insight into the mode of binding of this compound into the active site of COX-2 led us to the understanding that subtle derivatization in a particular position(s) might reveal a novel series of inhibitors. It was noticed that, though impatiently binds to the same site as occupied by inhibitor celecoxib in PDB 3LN1, yet there is an unoccupied site surrounded by Tyr341, Arg106, Leu517, Ile313, Leu345 and Val102 (Figure 2). This vacant site seemed to be an area of derivatization of this particular compound. Tyr341 and Arg106 could be treated as a site of charge-charge interactions whereas the rest comprise a hydrophobic site.

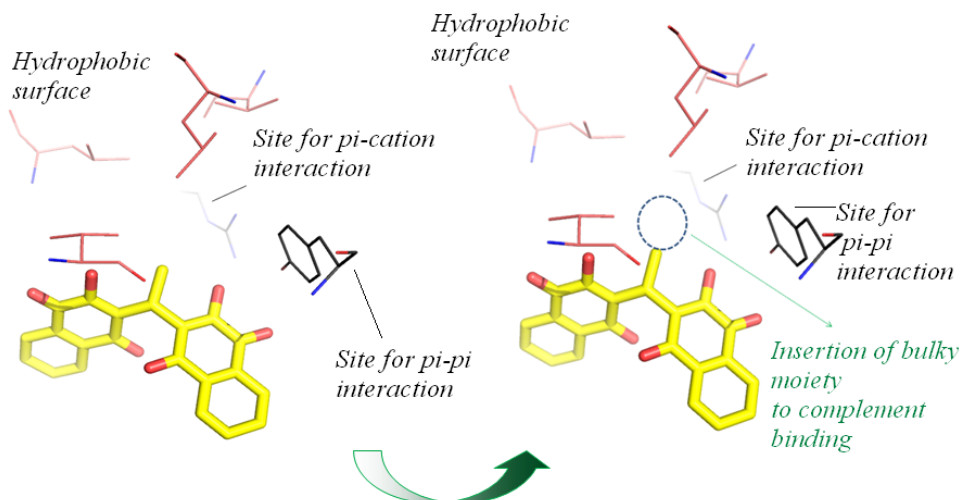


Figure 2. Identification of site for molecular modification on imatienol

Materials and Methods

Chemicals

All chemicals used in this work were purchased from Sigma Aldrich Chemical Company. Lawsone was obtained from Sigma Aldrich, Bangalore, India. Solvents were used as obtained from the supplier (Merck Chemical Company) or redistilled as necessary. Thin-layer chromatography was performed on ready-made sheets from Merck Chemical Company. Melting points were measured on the capillary melting point apparatus and were uncorrected. Mass spectra were recorded on a QSTAR Q-TOF Ab Sciex corporation, Ontario, Canada. ^1H NMR spectra and ^{13}C NMR were recorded in DMSO with 400 MHz on a BRUKER advanced liquid state NMR using Trimethylsilane as an internal standard and the chemical shifts (δ) are reported in ppm. IR spectra (KBr discs) were recorded on a SHIMADZU FT-IR 8400-S spectrophotometer.

Chemistry

General procedure for the preparation of 3, 3'-(arylmethylene) bis (2-hydroxynaphthalene-1, 4-dione) (1-10)

A mixture of lawsone (1mmol), aldehyde (1mmol), and amino acid ester (1mmol) in methanol/ethanol (5 mL) was stirred for 30 minutes to 24 hrs at room temperature and the progress of the reaction was monitored by thin-

layer chromatography. After completion of the reaction, the reaction mixture was filtered and the precipitate was washed with water and methanol. The compounds 1-10 were recrystallized from hot methanol/ethanol to afford the pure product. Amino acid ester was used as a catalyst. The reaction was performed with other amines but some amines are given a mixture of dimer or monomer. KOH was used for the reaction but no product was formed in presence of KOH. We used different amino acid ester for the reaction but only phenylalanine and tryptophan were found good for reaction giving better yield in Scheme 1 (Figure 3).

Physico chemical data of the products

3,3'-(3,4,5-tri-methoxyphenyl)methylene) bis (2-hydroxynaphthalene-1,4-dione) (1). Yellow powder, mp 178-180 °C; IR (KBr) (ν_{max} , cm^{-1}): 3335, 2944, 2846, 1670, 1590, 1038 cm^{-1} ; ^1H NMR (DMSO- d_6): δ_{H} 3.62 (s, 3H, OCH_3), 6.04 (s, 2H, CH), 6.51 (s, 2H, H-Arom), 7.74-7.98 (8H, m, H-Arom) ppm; ^{13}C NMR (DMSO): 25.0, 37.5, 55.8, 59.8, 66.9, 105.9, 123.0, 125.4, 125.9, 129.9, 132.2, 132.9, 134.5, 135.7, 136.4, 152.2, 156.7, 181.3, 183.4 ppm; MS (Mass) m/z : 526[M+H].

3,3'-(4-dimethylaminophenyl)methylene) bis (2-hydroxynaphthalene-1, 4-dione) (2). Brown red powder, mp 198-200 °C; IR (KBr) (ν_{max} , cm^{-1}): 3498, 3333, 2919 2850, 1670, 1599, 1346 cm^{-1} ; ^1H NMR (DMSO- d_6): δ_{H} 3.33 (s, 1H, CH_3), 6.26 (s, 1H, CH), 6.76 (s, 1H,

H-Arom), 7.06 (d, 2H, H-Arom), 7.71- 7.95 (m, 8H, H-Arom) ppm ; ^{13}C NMR (DMSO): 32.0, 112.4, 122.9, 124.9, 125.6, 127.3, 129.2, 130.9, 131.7, 133.3, 133.6, 148.1, 164.5, 182.3, 183.7 ppm ; MS (Mass) m/z: 480 [M+H].

3,3'-(4-hydroxy-3-methoxy phenyl)methylene bis (2-hydroxynaphthelene-1,4-dione) (3). Reddish brown powder, mp 180-182°C; IR (KBr) (ν max, cm^{-1}) : 3326, 2920, 2842, 1673, 1585, 1033 cm^{-1} ; ^1H NMR (DMSO- d_6) : δ_{H} 3.65 (s, 1H, OCH₃), 5.94 (s, 1H, CH), 6.61 (d, 2H, H-Arom), 6.81 (s, 1H, H-Arom), 7.76-8.00 (m, 8H, H-Arom) ppm ; ^{13}C NMR (DMSO) : 25.0, 37.02, 55.6, 66.9, 113.0, 114.6, 120.4, 123.6, 125.4, 125.9, 129.8, 131.2, 132.2, 132.9, 134.5, 144.6, 146.9, 156.1, 181.2, 183.6 ppm; MS (Mass) m/z : 482 [M+H].

3,3'-((4-Chlorophenyl)methylene)bis(2-hydroxynaphthalene-1,4-dione)(4). Orange powder, mp 180-182 °C ; IR (KBr) ($\nu_{\text{max}}, \text{cm}^{-1}$): 3337, 1674, 1597 cm^{-1} ; ^1H NMR (DMSO- d_6): δ_{H} 3.90 (bs, OH, overlap with solvent), 6.60 (s, 1H, CH), 7.11-7.96 (m, 12H, Arom.) ppm; ^{13}C NMR (DMSO- d_6): 37.6, 123.0, 126.0, 126.4, 127.9, 130.3, 130.4, 130.5, 132.6, 133.5, 135.1, 140.5, 156.8, 181.6, 183.9 ppm; MS (Mass) m/z : 470 [M+H].

3,3'-((4-Cyanophenyl)methylene) bis (2-hydroxynaphthalene-1,4-dione) (5). Orange yellow powder, mp 195-197 °C; IR (KBr) (ν max, cm^{-1}): 3510, 2901, 2229, 1674, 1597 cm^{-1} ; ^1H NMR (DMSO- d_6): δ_{H} 3.30 (bs, OH, overlap with solvent), 6.72 (s, 1H, CH), 7.31-7.97 (m, 12H, Arom) ppm; ^{13}C NMR (DMSO- d_6): 33.6, 107.5, 119.2, 121.4, 125.1, 125.7, 127.9, 130.9, 131.6, 131.9, 131.1, 133.7, 148.1, 182.2, 183.2 ppm; MS (Mass) m/z : 461 [M+H].

3,3'-((3,4,di-methoxyphenyl)methylene)bis(2-hydroxynaphthelene-1,4-dione)(6). Red powder, mp 185-187 °C; IR (KBr) ($\nu_{\text{max}}, \text{cm}^{-1}$) : 3335, 2944, 2846, 1674, 1550, 1338, 1038 cm^{-1} ; ^1H NMR (DMSO- d_6) : δ_{H} 3.67 (s, 3H, OCH₃), 6.04 (s, 1H, CH), 6.60 (t, 2H, CH), 6.70 (s, 2H, CH), 7.62-7.98 (m, 8H, H-Arom) ppm; ^{13}C NMR (DMSO): 32.5, 55.4, 111.4, 111.5, 119.0, 122.0, 125.6, 130.9, 131.7, 133.3, 133.6, 146.5, 148.2, 183.0 ppm. MS (Mass) m/z: 496.12 [M+H].

3,3'-(phenylmethylene)bis(2-hydroxynaphthelene-1,4-dione) (7). Yellow powder, mp 202-204 °C; IR (KBr) (ν max, cm^{-1}): 3336, 1660, 1587 cm^{-1} ; ^1H NMR (DMSO- d_6) : δ_{H} 6.25 (s, 1H, CH) 7.26-7.78 (m, 13H, Arom) 8.08-8.11 (m, OH) ppm; ^{13}C NMR (DMSO): 38.8, 123.0, 125.3, 125.4, 125.9, 127.5, 128.0, 129.8, 132.2, 132.9, 134.5, 140.8, 181.3, 183.4 ppm ; ESI-MS, m/z: 436.09 (M+1)

3,3'-((4-vinyloxy)phenyl)methylene)bis(2-hydroxynaphthelene-1,4-dione) (8). Yellow powder, mp 220-222 °C; IR (KBr) ($\nu_{\text{max}}, \text{cm}^{-1}$): 3433, 2939, 1658, 1604, 1435, 1334, ^1H NMR (DMSO- d_6) : δ 4.51 (d, 1H, CH) 5.30 (t, 1H, CH) 5.43 (d, 1H, CH), 6.00 (s, 1H, CH), 6.80 (d, 1H, CH), 7.20 (d, 1H, CH), 7.5 (s, 1H, CH), 7.90-8.5 (m, 8H, H-Arom); ^{13}C NMR (DMSO): 22.0, 68.6, 69.0, 114.6, 118.0, 124.3, 126.3, 126.8, 127.4, 127.8, 129.6, 129.9, 130.0, 130.8, 131.2, 133.8, 134.3, 134.9, 135.4, 135.7, 146.4 ppm.

3,3'-((4-fluorophenyl)methylene)bis(2-hydroxynaphthalene-1,4-dione) (9). Red powder, mp 200-205°C; IR (KBr) ($\nu_{\text{max}}, \text{cm}^{-1}$): 3471, 1666, 1597 cm^{-1} ; ^1H NMR (DMSO- d_6): δ_{H} 3.31 (bs, OH, overlap with solvent), 6.64 (s, 1H, CH), 7.00-7.96 (m, 12H, Arom) ppm; ^{13}C NMR (DMSO- d_6): 32.3, 111.9, 114.1, 114.3, 122.3, 125.0, 128.4, 128.5, 130.9, 131.8, 133.2, 133.7, 137.3, 159.1, 161.0, 183 ppm; MS (Mass) m/z : 453 [M+H].

3,3'-(thiophen-2-yl methylene) bis (2-hydroxy-2, 3-dihydro naphthalene-1,4-dione) (10). Mustard yellow powder, mp 226-228 °C; IR (KBr) ($\nu_{\text{max}}, \text{cm}^{-1}$): 3400, 1674, 1590 cm^{-1} ; ^1H NMR (DMSO- d_6): δ_{H} 3.50 (bs, OH, overlap with solvent), 3.82 (s, 1H, CH), 4.00 (t, 2H, CH) 5.25 (t, 2H, CH), 6.83 (d, 1H, CH), 6.93 (t, 2H, CH), 7.40 (d, 1H, CH), 8.5 (s, 8H, Arom) ppm; ^{13}C NMR (DMSO- d_6): 24.5, 51.6, 70.0, 124.9, 125.1, 125.8, 126.4, 133.0, 144.5, 185.0 ppm. MS (Mass) m/z : 442.05 [M+H].

Surface plasmon studies

Methodology

Kinetic measurement of the interaction between protein COX-2 with ligands (Compound 1-10) [Figures shown in Supplementary material] was performed using a biosensor based on surface plasmon resonance (SPR). The interaction phenomenon of two biological molecules can be monitored directly by the SPR. The phenomenon of SPR was studied by Otto [1] and Kretschmann and Raether [2] and it was used as a chemical detection method by Nylander et al. [3]. An automatic instrument BIAcore 2000 (Pharmacia Bioscience) was used. Experiments were performed at 25°C in HBS-P buffer containing 10 mM HEPES (pH 7.4), 150 mM NaCl, 50 μM EDTA and 0.005% P20 (surfactant).

Six histidine-tag attached to the terminal position of protein is an ideal tag for immobilization due to the strong rebinding effect caused by the high surface density of immobilized N²⁺-nitroacetic acid (NTA) on the chips used here, i.e. the binding of analyte (1-10) in the solution can be studied by monitoring the change in the resonance unit (RU) values of the sensorgram, where the progress of the interaction is plotted against time, revealing the binding characteristics. Analysis of binding kinetics, that is the association (K_A) and dissociation (K_D) constant for the formation of multi-molecular complex and dissociation, was done in a very short time and with a small number of samples. The flow cells of the chips were activated by passing Nickel chloride solution over them. 40 microliters of His-protein; (50 μg/mL) were injected into one of the flow cells at the flow rate of 5 μL/min. Nine hundred resonance unit (RU) of COX-2 was immobilized under these conditions, where 1 RU corresponded to an immobilized protein concentration of 1 pg/mm² [4]. Three different concentrations of compound 1 were passed over the immobilized proteins at the flow rate of 10 μL/min and the sensorgram was run for 4 min. After passing each concentration, the regeneration was done by 1 mM NaOH solution. The change in

sensorgram was observed. The graph shows the change in RU values with time for different concentrations of Compound 1. The rate constants K_A and K_D were obtained by fitting the primary sensorgram data using the BIA evaluation v3.0 software. Similarly, all compounds (1-10) at three different concentrations were passed through all proteins and the same protocol was observed as mentioned above.

Molecular docking studies

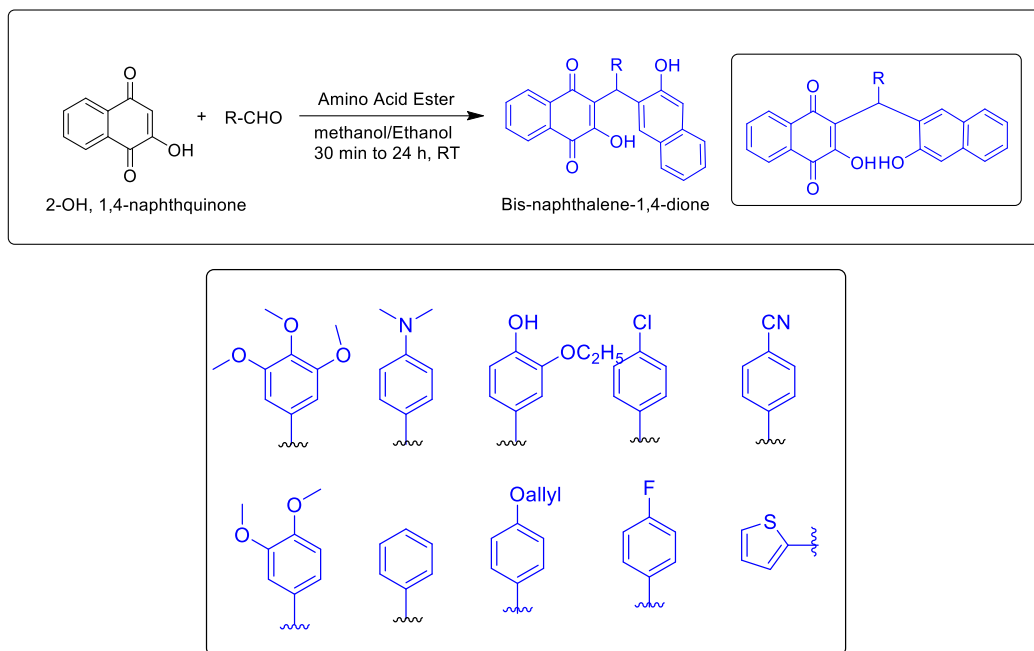
Multiple receptor models were generated using MRC webserver (<http://abagyan.ucsd.edu/MRC>) [5] with COX-2 crystal structure PDB Id: 3LN1 [6]. The sphere radius of 8 Å around the neighboring residues surrounding the co-crystallized ligand was taken as a site of multiple model development. The rest of the parameters were accepted as the default. Total eighteen models were generated. Autodock Vina [7] with PyRx software [8] was used as a docking program. AutoDock Vina combines some advantages of knowledge-based potentials and empirical scoring functions; it extracts empirical information from both the conformational preferences of the receptor-ligand complex and from experimental affinity measurements. Ligands are ranked based on an energy scoring function and, to speed up the score calculation, grid-based protein-ligand interactions are used. In all the docking calculations, the docking site was defined by a cube containing Val105, Trp373, Leu 370, Tyr371, Phe367, Met508, Phe504, Gly512, Ser516, Ala513, Val509, Arg106, Val335, Leu338, Ser339, Gly340, Arg499, Ala502, Gln178, Leu345, Tyr341, Val335, Ile503, His75 and Leu517. Only the best score-related poses were considered for further analysis. Pymol [9] Molegro Molecular Viewer [10] and Discovery Studio visualizer 3.5 were used for molecular visualization and analysis.

Results and Discussion

Recently, this class of compounds has been synthesized by AyoobBazgir and co-workers [11]. The major disadvantage we faced during the repetition of the synthesis using water as

solvent was the stickiness of the reactants during the progress of the reaction which sometimes led to incomplete reactivity. As an alternative approach, to explore the possibility of amino acids as catalysts in this reaction, we tested phenylalanine and tryptophan esters. The precipitation of desired compounds started

almost immediately and in all the cases, analytically pure products were obtained as the reaction was over by few hours with high yield. The mechanism of conversion of Lawsone to compound **3**, **3'-(arylmethylene) bis (2-hydroxynaphthalene-1, 4-dione)** is believed to proceed through two consecutive steps.



Scheme 1. Synthesis of Bis-naphthalene-1,4-dione

1. The amine catalyzed aldol condensation between aldehyde and lawsone (i-viii).

2. Amine catalyzed Michael addition between aldol condensation product and 2nd molecule of lawsone (ix-xi). To catalyze both steps, lawsone requires the formation of enamine intermediate on reaction with phenylalanine. The mechanism is outlined in the following scheme. (**See Figure in Supplementary material**).

Lawsone reacted with phenylalanine ester to give imine, which was eventually isomerized to enamine derivative. The enamine derivative underwent aldol addition with the aldehyde to give aldol product, which further dehydrated efficiently to condensation product as the β -hydrogen possess an acidic nature. After this step, regenerated amine reacted with another molecule of lawsone to give enamine, which further catalyzed Michael's addition (1,4-addition) to give the final molecule.

Kinetic measurement of the interaction between COX-2 with ligands (1-10), standard drugs diclofenac and nimesulide were performed using a biosensor based on surface plasmon resonance (SPR). The interaction phenomenon of two biological molecules was monitored directly by the SPR. The SPR studies involve immobilization of one interacting partner onto the surface of a sensor chip, while the other flowed over the surface in solution. Interaction between the two generated a response that was proportional to the bound mass. The resonance angle expressed in the resonance unit (RU) depends on the refractive index of the vicinity of the surface and changes with the concentration of the molecules on the surface. The SPR technique provides accurate detection of the analyte at the pico and nano-molar range. The results of the binding experiment can be found in **Table 1**.

Enzyme binding studies

Table 1. Dissociation constant of 3,3'-(arylmethylene) bis (2-hydroxynaphthalene-1,4-dione) derivatives from compounds 1 to 10

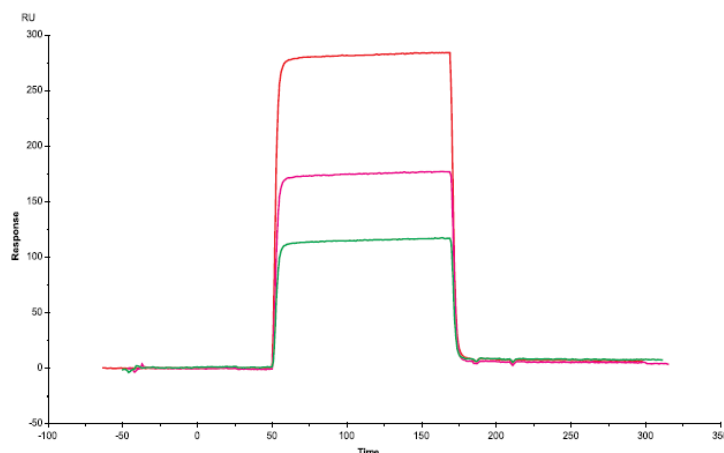
Compound no.	Kd(M)*
1	1.25×10^{-7}
2	8.45×10^{-6}
3	7.04×10^{-7}
4	2.30×10^{-6}
5	5.52×10^{-6}
6	2.91×10^{-7}
7	1.18×10^{-7}
8	9.42×10^{-7}
9	1.25×10^{-6}
10	1.97×10^{-10}
Diclofenac**	1.45×10^{-7}
Nimesulide**	2.22×10^{-9}

*Kd= Dissociation constant in molar

**Diclofenac and nimesulide used as a standard inhibitor

As expected, all the compounds were found active against the protein target with compound-10 showing considerably high activity with K_D of $1.97 \times 10^{-10} \text{M}$ (Figure 4). The presence of sulfur atom and its effect on COX-2 inhibition has been previously noted with the small molecules like the coxib class of drugs and nimesulide as well as with peptide

inhibitors like FCS, WCS and WCY as recently published by Sharmistha Dey and co-workers. Likewise, in the present case, compound-10, which bears a thiophene ring also demonstrated a sharp increase in COX-2 inhibition characteristics compared with the rest of the compounds, including standard drugs.

**Figure 4.** The graphical representation of the change in RU (resonance unit) values with time

Molecular docking studies

Molecular docking studies have been conducted keeping receptor flexibility into consideration. It has been proved time and again with experimental and theoretical evidence showing that proteins move at room (or physiological) temperature and rearrange in response to binding [12-15]. Computational generation of

receptor ensembles can be achieved by two vastly accepted methods, namely, computationally expensive molecular dynamics simulations and Normal Mode Analysis (NMA). For inclusion of the protein flexibility, the current work considers the utilization of ensembles of structures, namely Multiple Receptor Conformations (MRCs) as the most promising alternative, where the ligand is

docked not to just one receptor conformation, but to a set of receptor conformations [16]. There is evidence [17-19] of molecular docking-based NMA generated receptor ensembles in the literature.

As mentioned in earlier sections, the conceptual genesis of the current work primarily targeted Leu517, Leu345 and Val102 along with Tyr341 and Arg106 as a probable site of hydrophobic and charge-charge interactions, respectively. The docking results revealed that the ligand occupies accordingly the same pocket as it was observed initially by

impatience. The thiophene ring of the ligand positions itself in the hydrophobic sub-pocket surrounded by Leu517, Leu345, and Val102 (Figure 5A). The other two naphthoquinone rings interact with the already established hydrophobic sites. In line with our initial assumption, consistent pi-pi and pi-cation interactions of the ligand were observed with different conformations of Tyr341 and Arg106 (Figure 5B). The docking results show that hydrogen bonds also do exist between compound 10 and Tyr341, Ser516, Tyr371, Arg499 and Arg106 with respective receptor models (Figure 6).

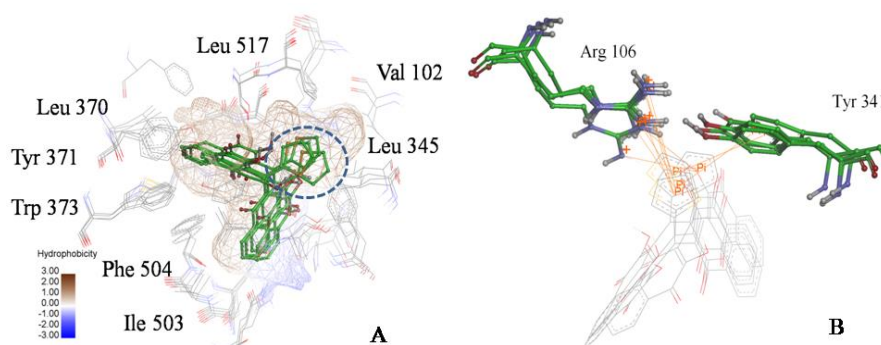


Figure 5. [A] The hydrophobic interaction of the ligand 10 with different ensembles of the hydrophobic sub-pocket surrounded by Leu517, Leu345 and Val102. [B] The charge-charge interactions of the ligand 10 with different ensembles of the binding site

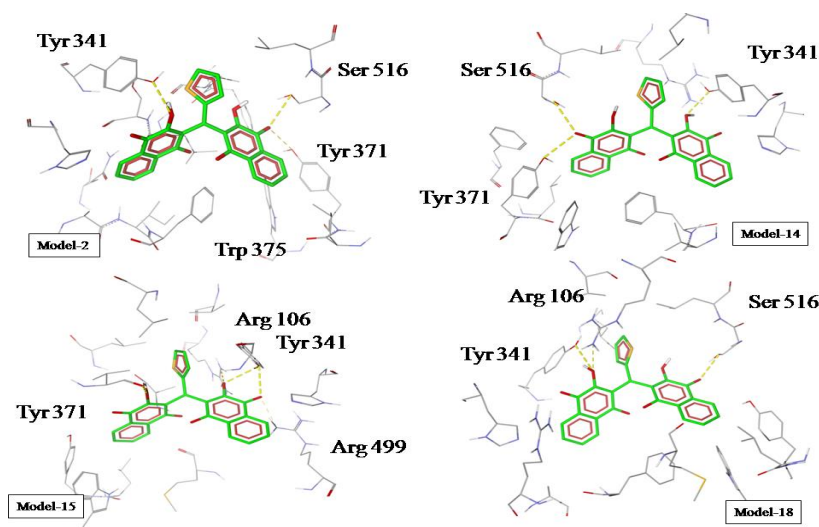


Figure 6. The hydrogen bond interactions of the ligand 10 with the different ensembles of the binding site

Conclusion

In summary, the current study describes the design of ten analogs of impatienol, which were synthesized subsequently and evaluated against cyclooxygenase-2, which is an established therapeutic target for inflammation as well as various cancers. The structure-based design has been done utilizing Multiple Receptor Conformations (MRCs), where the ligand is docked not to just one receptor conformation, but rather to a set of receptor conformations. Excellent binding was observed for compound **10** ($K_D = 1.97 \times 10^{-10} \text{M}$) when a kinetic measurement of the interaction between COX-2 with ligands (**1-10**) was performed using a biosensor based on surface plasmon resonance (SPR) with BIAcore instrument. The results also demonstrated that the designed compounds are better than standard drugs like diclofenac and nimesulide in binding the enzyme. The docking results revealed that the thiophene ring of the ligand occupies the hydrophobic sub-pocket surrounded by Leu517, Leu345 and Val102, and consistent pi-pi and pi-cation interactions of the ligand were observed with different conformations of Tyr341 and Arg106 which were understood to be deciding factors in strong binding. Future research may address evaluating the specificity of this class of compounds as well as on in-vivo models of inflammation.

Acknowledgment

GS and SB thank the management and administration of Motherhood University for their encouragement and support.

Declaration of interests

The authors report no declarations of interest.

Symbols and abbreviations

COX-2, Cyclooxygenase-2; SPR, Surface Plasmon resonance; NMA, Normal Mode Analysis)MRCs, Multiple Receptor Conformations; K_D , Dissociation constant; HEPES (4-(2-hydroxyethyl)-1-piperazineethanesulfonic acid;

RU, Resonance Unit; NTA, N 2+-nitriloacetic acid.

Orcid:

Garima Sharma:<https://orcid.org/0000-0002-7151-3968>

S.B.Sharma:<https://orcid.org/0000-0003-4292-2161>

References

- [1] A. Otto, *Zeitschrift für Physik A Hadrons and nuclei*, **1968**, 216, 398–410. [[crossref](#)], [[Google Scholar](#)], [[Publisher](#)]
- [2] E. Kretschmann, H. Raether, *Verlag der Zeitschrift für Naturforschung*, **2014**, 23, 2135–2136. [[crossref](#)], [[Google Scholar](#)], [[Publisher](#)]
- [3] R.K. Somvanshi, A. Kumar, S. Kant, D. Gupta, S.B. Singh, U. Das, A. Srinivasan, T.P. Singh, S. Dey, *Biochem. Bioph. Res. Commun.*, **2007**, 361, 37–42. [[crossref](#)], [[Google Scholar](#)], [[Publisher](#)]
- [4] M. Rueda, G. Bottegoni, R. Abagyan, *J. Chem. Inf. Model.*, **2009**, 49, 716–725. [[crossref](#)], [[Google Scholar](#)], [[Publisher](#)]
- [5] J.L.Wang, D. Limburg, M.J. Graneto, J. Springer, J.R. Hamper, S.Liao, J.L. Pawlitz, R.G. Kurumbial, T. Maziasz, J.J.Talley, J.R. Kiefer, J.Carter, *Bioorg. Med. Chem. Lett.*, **2010**, 20, 7159–7163. [[crossref](#)], [[Google Scholar](#)], [[Publisher](#)]
- [6] O. Trott, A.J. Olson, *J. Comput. Chem.*, **2010**, 31, 455–461. [[crossref](#)], [[Google Scholar](#)], [[Publisher](#)]
- [7] A.G. Asting, A. Farivar, B.-M. Iresjö, H. Svensson, B. Gustavsson, K. Lundholm, *BMC Cancer*, **2013**, 13, 511. [[crossref](#)], [[Google Scholar](#)], [[Publisher](#)]
- [8] The PyMOL Molecular Graphics System, Version 1.3r1 edu (Sept 2010) Schrödinger, LLC.
- [9] R. Thomsen, M.H. Christensen, *J. Med. Chem.*, **2006**, 49, 3315–3321. [[crossref](#)], [[Google Scholar](#)], [[Publisher](#)]
- [10] Z.N. Tisseh, A. Bazgir, *Dyes and Pigments*, **2009**, 83, 258–261. [[crossref](#)], [[Google Scholar](#)], [[Publisher](#)]
- [11] K.A. Henzler-Wildman, M. Lei, V. Thai, S.J. Kerns, M. Karplus, D. Kern, *Nature*, **2007**,

- 450, 913–916. [[crossref](#)], [[Google Scholar](#)], [[Publisher](#)]
- [12] R. Ishima, D.A. Torchia, *Nat. Struct. Biol.*, **2000**, *7*, 740–743. [[crossref](#)], [[Google Scholar](#)], [[Publisher](#)]
- [13] O.F. Lange, N.A. Lakomek, C. Fares, G.F. Schroder, K.F. Walter, S. Becker, J. Meiler, H. Grubmuller, C. Griesinger, B.L. de Groot, *Science*, **2008**, *320*, 1471–1475. [[crossref](#)], [[Google Scholar](#)], [[Publisher](#)]
- [14] S.J. Teague, *Nat. Rev. Drug Discovery*, **2003**, *2*, 527–541. [[crossref](#)], [[Google Scholar](#)], [[Publisher](#)]
- [15] S.F. Sousa, P.A. Fernandes, M.J. Ramos, *Proteins. Struct. Funct. Bioinf.*, **2006**, *65*, 15–26. [[crossref](#)], [[Google Scholar](#)], [[Publisher](#)]
- [16] Q. Cui, I. Bahar, *FL*, **2006**, 406. *Mathematical and Computational Biology Series 9*. Chapman & Hall/CRC Press/Taylor & Francis, Boca Raton, FL, **2006** (406 pp.). ISBN 1-58488-472-X. [[Publisher](#)]
- [17] A. May, M. Zacharias, *J. Med. Chem.*, **2008**, *51*, 3499–3506. [[crossref](#)], [[Google Scholar](#)], [[Publisher](#)]
- [18] T. Sandera, T. Liljeforsa, T. Balle, *J. Mol. Graph. Model.*, **2008**, *26*, 1259–1268. [[crossref](#)], [[Google Scholar](#)], [[Publisher](#)]